Author Manuscript

Author Manuscript

Author Manuscript

Author Manuscript

HHS Public Access

Author manuscript

Clin Cancer Res. Author manuscript; available in PMC 2016 December 15.

Published in final edited form as:

Clin Cancer Res. 2015 December 15; 21(24): 5588–5600. doi:10.1158/1078-0432.CCR-14-3283.

Pre-clinical efficacy of Ron kinase inhibitors alone and in combination with PI3K inhibitors for treatment of sfRon-expressing breast cancer patient-derived xenografts

Magdalena Bieniasz[1,*], **Parvathi Radhakrishnan**[2], **Najme Faham**[1], **Jean-Paul De La O**[2,3], and **Alana L. Welm**[1,*]

[1]Oklahoma Medical Research Foundation, Program in Immunobiology and Cancer, Oklahoma City, Oklahoma

[2]University of Utah, Salt Lake City, Utah

Abstract

Purpose—Recent studies have demonstrated that short-form Ron (sfRon) kinase drives breast tumor progression and metastasis through robust activation of the PI3K pathway. We reasoned that upfront, concurrent inhibition of sfRon and PI3K might enhance the anti-tumor effects of Ron kinase inhibitor therapy while also preventing potential therapeutic resistance to tyrosine kinase inhibitors (TKIs).

Experimental design—We used patient-derived breast tumor xenografts (PDXs) as high-fidelity pre-clinical models to determine the efficacy of single agent or dual Ron/PI3K inhibition. We tested the Ron kinase inhibitor ASLAN002 with and without co-administration of the PI3K inhibitor NVP-BKM120 in hormone receptor positive (ER+/PR+) breast PDXs with and without *PIK3CA* gene mutation.

Results—Breast PDX tumors harboring wild-type *PIK3CA* showed a robust response to ASLAN002 as a single agent. In contrast, PDX tumors harboring mutated *PIK3CA* demonstrated partial resistance to ASLAN002, which was overcome with addition of NVP-BKM120 to the treatment regimen. We further demonstrated that concurrent inhibition of sfRon and PI3K in breast PDX tumors with wild-type *PIK3CA* provided durable tumor stasis after therapy cessation, whereas discontinuation of either monotherapy facilitated tumor recurrence.

Conclusion—Our work provides pre-clinical rationale for targeting sfRon in breast cancer patients, with the important stipulation that tumors harboring *PIK3CA* mutations may be partially resistant to Ron inhibitor therapy. Our data also indicate that tumors with wild type *PIK3CA* are most effectively treated with an upfront combination of Ron and PI3K inhibitors for the most durable response.

[*]Co-Corresponding Authors: Alana Welm and Magdalena Bieniasz, Oklahoma Medical Research Foundation, Department of Immunobiology and Cancer, 825 NE 13th St, Oklahoma City, OK 73104. Phone: 405-271-2155; alana-welm@omrf.org; magdalena-bieniasz@omrf.org.

[3]Current addres: Myriad Genetics, Salt Lake City, Utah

Disclosure of Potential Conflicts of Interest: ALW received grant funding from OSI Pharmaceuticals for research on various Ron inhibitory compounds. MB, PR, NF and JD declare that they have no conflicts of interest.

Author Manuscript Author Manuscript Author Manuscript Author Manuscript

Keywords

ASLAN002; NVP-BKM120; breast cancer; PDX; PI3K; Ron kinase inhibitor; Ron

Introduction

The Ron receptor tyrosine kinase and its ligand, macrophage simulating protein, have been shown to be upregulated in breast and other cancers, and the pathway is correlated with poor clinical outcome (1–3). We recently discovered that an alternative isoform of Ron, known as short-form Ron (sfRon), is also a significant contributor to breast cancer pathogenesis (4). sfRon is generated by alternative transcription from a second promoter within exon 10 of the *RON* gene (5). Thus, the sfRon protein lacks the N-terminus of Ron, including the ligand-binding domain, but organizes into a constitutively-active transmembrane protein with an intracellular amino acid sequence that is identical to full-length Ron (4). Our previous studies revealed the surprising discovery that the major active (phosphorylated) Ron isoform in patient-derived breast tumors is sfRon, rather than full-length Ron. In the same study, we also determined that sfRon plays a significant role in the aggressiveness of breast cancer *in vivo* by dramatically promoting tumor growth and metastasis (4). We found that sfRon signals strongly through PI3K, which was required for the tumor promoting and metastatic function of sfRon in MCF7 xenografts (4). Since sfRon protein is expressed in approximately 69% of breast tumors, with no detectable expression in healthy breast (4), sfRon may be a good target for breast cancer therapy.

The PI3K signaling network is frequently dysregulated in breast cancer (6). Mutations of *PIK3CA* gene, which encodes the p110α catalytic subunit of PI3K, are among the most frequent mutational events in breast cancer - occuring in 18% to 40% of tumors (7, 8). Almost all *PIK3CA* mutations involve “hotspots” on exons 9 and 20, corresponding to the helical (E542K and E545K) and kinase (H1047R) domain mutations, respectively (8, 9). These mutations result in elevated catalytic activity of p110α (10) and cause cell transformation (11). Importantly, molecular alterations within the PI3K pathway predict responsiveness to PI3K pathway-targeted agents (12, 13) and correlate with resistance to targeted therapy of upstream receptors (14–17).

Although breast cancer is among the most chemosensitive of the solid tumors, important improvements in survival have been achieved during the past two decades with the introduction of targeted therapies, which are generally better tolerated than cytotoxic chemotherapy (18). In pre-clinical studies, single agent Ron inhibitors have been reported to inhibit growth of colon, breast, and pancreatic tumor xenografts (19–23). Based on these pre-clinical data, Phase I clinical trials have been initiated with Ron inhibitors for multiple cancers (IMC-RON8, an inhibitory antibody in trial #NCT01119456; and ASLAN002, a Ron kinase inhibitor in trial #NCT01721148). However, none of the Ron inhibitory antibodies that have been developed (such as IMC-RON8) will block sfRon, which lacks most of the extracellular domain and does not require ligand binding for activity (4). Inhibition of Ron kinase activity with small molecules (such as ASLAN002), on the other

Author Manuscript Author Manuscript Author Manuscript Author Manuscript

hand, would block both Ron and sfRon and therefore might be a more efficacious approach in tumors where sfRon is expressed.

Pre-clinical drug testing largely relies on *in vitro* and xenograft assays to determine the efficacy of candidate anti-tumor agents. This system is suboptimal, as evidenced by common failures at the phase II and phase III stages of human testing due to lack of anti-tumor efficacy in humans (24, 25). Likewise, xenograft models using human breast cancer cell lines, despite their clear advantages for speed and ease of use, only partially recapitulate breast tumor biology, metastatic progression, and response to therapy - potentially resulting in poor predictions of drug performance (25–27). To best address challenges associated with reliability of tumor models for *in vivo* drug testing, we utilized our patient-derived orthotopic breast tumor xenograft (PDX) models, which retain characteristics of patient tumors with very high fidelity (28). Importantly, most of our PDX models, like bona fide human breast tumors (4), overexpress endogenous sfRon, which is consistently maintained through multiple rounds of serial transplantation of the PDX tumor.

Here, we report the *in vivo* efficacy of the Ron kinase inhibitor ASLAN002 with and without co-administration of the PI3K inhibitor NVP-BKM120 in (ER+/PR+) breast PDX models. The study results validate Ron and PI3K pathway inhibitors as potential targeted therapy for breast cancers overexpressing sfRon. Our data also indicate the importance of considering *PIK3CA* mutation status in the setting of Ron inhibition.

Materials and Methods

Source of cells and tumors

MCF7 cells expressing sfRon (MCF7-sfRon) were previously described (4). Our MCF7 cell lines were authenticated by short tandem repeat (STR) profiling analysis by ATCC on 01/05/2015. Our MCF7 cell lines are an exact match to ATCC cell line HTB-22 (MCF7). HCI-002, HCI-003, HCI-007, HCI-011, and HCI-013 PDX tumors were obtained from our published collection (28, 29) and implanted as tumor fragments into cleared inguinal mammary fat pads as described below and in our detailed protocol paper (30).

Generation of lentiviruses and cell transduction

To generate breast cancer cell lines expressing sfRon and the most common mutations of the *PIK3CA* gene found in breast tumors, the endogenous *PIK3CA* gene was knocked down in MCF7-sfRon cells, followed by conditional re-expression of different variants of this gene (WT, E545K or H1047R). The knockdown was performed by lentiviral transduction of MCF7-sfRon cells using lentiviral plasmid pLKO.1-puro shRNA directed against 3′-UTR of the *PIK3CA* gene (Sigma-Aldrich; validated MISSION shRNA clone, TRCN0000010407, clone ID NM_006218.x-3234s1c1) followed by selection with puromycin. To conditionally re-express variants of *PIK3CA* gene, MCF7-sfRon *PIK3CA* knockdown cells were subsequently transduced with pLentiTRE/rtTA-*PIK3CA*^{WT}, pLentiTRE/rtTA-*PIK3CA*^{E545K} or pLentiTRE/rtTA-*PIK3CA*^{H1047R} lentiviruses, which were constructed as follows: The coding sequence of the wild-type *PIK3CA* gene was amplified by PCR from pBabe puro HA *PIK3CA* plasmid (plasmid 12522, Addgene) and flanked by restriction sites for the HpaI and

Author Manuscript Author Manuscript Author Manuscript Author Manuscript

PacI enzymes. Next, the sequence was sub-cloned into HpaI and PacI restriction sites of the tetracycline inducible (Tet-On) lentiviral expression vector pLentiTRE/rtTA carrying both TRE and rtTA cassettes (kindly provided by Trudy Oliver, Huntsman Cancer Institute, Salt Lake City, UT). Specific mutations were introduced into the WT *PIK3CA* sequence by site-directed mutagenesis with the QuikChange Site-Directed Mutagenesis Kit (Stratagene). Primers used to generate the desired mutation were (mutated nucleotide in bold):

E545K-Fwd: CTCTGAAATCACT**A**AGCAGGAGAAAGATTTTCTATGGAGTC

E545K-Rev: GACTCCATAGAAAATCTTTCTCCTGCT**T**AGTGATTTCAGAG

H1047R-Fwd: ATGAATGATGCAC**G**TCATGGTGGCTGGACAACAAAAATGG

H1047R-Rev: CCATTTTTGTTGTCCAGCCACCATGA**C**GTGCATCATTCAT

The presence of the correct mutation was verified by sequencing. Recombinant lentiviruses were produced in HEK293T cells according to standard protocols (31). MCF7-sfRon sh*PIK3CA* cells were then infected with lentiviruses containing the tetracycline-inducible *PIK3CA* variants, followed by selection with blasticidin. Rescued PI3K expression in MCF7-sfRon sh*PIK3CA* cells was induced by the addition of 500 ng/ml of doxocycline (DOX) for 24 h.

Drugs and reagents

Doxycycline was purchased from Sigma-Aldrich (St Louis,. MO) and dissolved in water to final concentration of 1 mg/ml. IMC-RON8 was provided by ImClone LLC system (New York, NY), diluted in PBS and 40 mg/kg dose was administered by IP injections 3 days a week. OSI-296 was obtained from OSI Pharmaceuticals and diluted in 40% Trappsol followed by sonication. For *in vivo* studies, OSI-296 was administered orally as a 200 mg/kg dose every other day. NVP-BEZ235 and NVP-BKM120 were provided by Novartis Pharmaceuticals. Lyophilized NVP-BEZ235 or NVP-BKM120 was dissolved in 1 volume of NMP (1-methyl-2-pyrrolidone, Sigma-Aldrich). After dissolution, 9 volumes of PEG300 (Sigma-Aldrich) was added to a final ratio of NMP 10%/PEG300 90%. Drug solutions (NVP-BKM120 at 60 mg/kg, or NVP-BEZ235 at 45 mg/kg) were administered orally to mice within 30 minutes to avoid precipitation. ASLAN002 was provided by ASLAN Pharmaceuticals and was prepared as a 500 mg/ml stock solution in DMSO. For *in vivo* experiments, mice were treated orally with a 50 mg/kg dose every other day. For *in vitro* studies, a 10 mM stock solution of each compound was made in DMSO and administered to cells at the concentrations indicated. Target inhibition was validated in MCF7-sfRon cells by first serum-depriving (0.5% FBS) for 24 h, then incubating with the appropriate inhibitor for 1 h, followed by cell lysis and examination of target protein phosphorylation.

Western blots and immunoprecipitations

Cells or tumors were lysed in Buffer B (25 mM Tris-HCl, pH 7.5, 0.42 M NaCl, 1.5 mM $MgCl_2$, 0.5 mM EDTA, 1 mM DTT, 25% sucrose, 1 mM Na_3VO_4, and 1X protease inhibitor cocktail) on ice for 15 min, followed by centrifugal clearing at 4°C for 10 min at 10,000 rpm to recover whole cell lysates. For immunoprecipitations, 200 μg whole cell lysate was diluted in IP buffer (50 mM Tris-HCl, pH 7.5, 150 mM NaCl, 1% (w/v) Triton

Author Manuscript Author Manuscript Author Manuscript Author Manuscript

X-100, 10% glycerol, 1 mM EDTA, 1 mM dithiothreitol, 1 mM Na_3VO_4, and 1X protease inhibitor cocktail) and immunoprecipitated by incubating with 30 µl of clone 4G10 anti-phosphotyrosine agarose conjugate (cat. no. 05-777, Millipore Co., Billerica, MA) for 16 h at 4°C. Immunoprecipitates were washed extensively with IP buffer, then processed for SDS-PAGE analysis and Western blotting. For Western blots, cellular proteins (100 µg whole cell lysate) were separated by 10% SDS-PAGE under reduced conditions and transferred to PVDF membranes (Millipore Co., Billerica, MA). Primary antibodies used were: anti-Ron (cat. no. sc-322; 1:500) from Santa Cruz Biotechnology (Santa Cruz, CA); anti-pan Akt (cat. no. 4691; 1:1000), anti-phospho Akt Ser473 (cat. no. 9271; 1:1000), anti-phospho-PRAS40 Thr246 (cat. no. 2997; 1:1000), anti-PRAS40 (cat. no. 2610; 1:2000), anti-PI3 Kinase p110 alpha (cat. no. 4249; 1:1000) from Cell Signaling Technology (Danvers, MA); and anti-β-actin (cat. no. ab6276; 1:1000) from Abcam (Cambridge, MA). Anti-rabbit or anti-mouse secondary antibodies, conjugated with horse radish peroxidase (Santa Cruz, CA) were applied, and specific bands were visualized using Western Lightning® Plus-ECL (PerkinElmer). Levels of chemiluminescence were captured and quantified with the ChemiDoc XRS system with Image Lab Software.

Dose response assays

The *in vitro* dose response assays were carried out by treating exponentially growing cells with the drugs followed by an MTT assay to measure cell viability using the Quick Cell Proliferation Assay kit II (BioVision, Milpitas, CA). Briefly, cells were seeded in a 96-well plate in 100 µL of their respective media at a density of 25,000 or 50,000 cells/well to achieve ~40% confluency (low cell culture density) or ~80% confluency (high cell culture density), respectively, after 3 days in culture. After cells were cultured for 3 days, the media were aspirated and cells were exposed to serial dilutions of drugs (concentrations ranging from 0.1 to 100 µM as indicated) for 4 days. In addition, a vehicle control corresponding to the highest DMSO concentration, which did not exceed 0.2%, was also included. Next, cells were incubated with the WST reagent for 2 h and absorbance was determined at 450 nm. Absorbance measurements were normalized to the DMSO control wells. Normalized values were plotted as an average ± SD of three wells per condition and these data were analyzed using the dose response nonlinear curve fitting function with GraphPad Prism 6.0 to determine the half maximal effective concentration (EC50).

Animal experiments

All animal procedures were approved by the University of Utah or Oklahoma Medical Research Foundation Institutional Animal Care and Use Committee. For tumor growth inhibition experiments, 4 to 6 week-old female NOD/SCID mice (stock #1303, Jackson Laboratory) were implanted subcutaneously with estrogen pellets (beeswax E2 pellets, each containing ~1 mg estrogen (Estradiol (1,3,5{10}-Estratriene-3, 17 β-diol), described in (30) and characterized in Supplementary Fig. 1) behind the shoulder blades, followed immediately by implantation of tumor cells or fragment into the right cleared inguinal mammary fat pad. Tumors consisted either of injection with 1×10^6 MCF7-sfRon cells suspended in Matrigel or implantation of a PDX fragment using our routine procedures (28, 30). Five PDXs with different clinical attributes were used in this study: HCI-002 [low/negative Ron and sfRon, *PIK3CA*^{WT}], HCI-003 [high sfRon, high *PIK3CA*^{H1047R}], HCI-007

Author Manuscript Author Manuscript Author Manuscript Author Manuscript

[high sfRon, *PIK3CA*^{WT}], HCI-011 [low sfRon, *PIK3CA*^{WT}] or HCI-013 [high sfRon, *PIK3CA*^{H1047R}]. Mice with established tumors of approximately 100 to 200 mm^3 volumes were randomized and then treated with the indicated drug regimen. A detailed summary of treatment doses, schedules and number of animals in each experiment is given in Supplementary Table 1. Tumor dimensions were measured with vernier calipers and tumor volumes were calculated using the formula ½ (Length × $Width^2$). Experiments involving PDXs were divided into two phases: a 4 week treatment phase followed by discontinuation of treatment and a 3 week observation phase to assess recurrence. At the end of the experiment, tumor specimens were harvested and snap-frozen in liquid nitrogen or fixed for further histological and molecular analysis.

Pharmacodynamic (PD) analysis of tumor specimens

To determine whether ASLAN002 and/or NVP-BKM120 therapy caused effective target inhibition in tumor tissue after 2 weeks of treatment, one animal from each treatment group (50 mg/kg of ASLAN002 and/or 60 mg/kg of NVP-BKM120) or vehicle (70% PEG in PBS) was euthanized three hours after routine drug administration. Tumors were harvested and analyzed by Western blotting for levels of phosphorylated target protein (p-sfRon, pAKT or pPRAS40) as previously described (32).

Morphologic and Immunohistochemical (IHC) analyses of tumors

Tumor sampling from treated PDXs was performed 3 h after the last drug treatment. Harvested tumors were fixed in 10% neutral buffered formalin, paraffin embedded, and hematoxylin–eosin (H&E) stained according to standard protocols by the Cancer Tissue Pathology core at the Stephenson Cancer Center, University of Oklahoma Health Science Center. Tumors were analyzed by IHC for expression of the following markers: anti-human cytokeratin (1:400, DAKO #Z0622), Ki67 (1:200, Thermo Scientific #RM-9106-S1) or cleaved caspase-3 (1:250, Cell Signaling #9661). Staining was visualized by 3,3-diaminobenzidine, with hematoxylin as a counter-stain. Slides were imaged on an Olympus Bx50 microscope with a Canon EOS Rebel XSI camera using EOS imaging software. For Ki67 or cleaved caspase-3 quantification, 4 images per one tumor from each treatment group were manually analyzed with ImageJ software, version 1.48v and Java 1.6.0_20 (32-bit) engine (33). The percentage of Ki67 or cleaved caspase-3 positive cells was quantified by the average ratio of positive nuclei to total nuclei in each field.

Statistical analysis

All *in vitro* experiments were performed three separate times and in triplicate when applicable. Analysis of tumor growth inhibition and comparison of the percentage of Ki67 or cleaved caspase-3 positive cells between groups was done using multiple t-test with Holm-Sidak correction. Error bars represent SEM. P values of less than 0.05 were considered significant. Statistical analysis was performed using GraphPad Prism 6.0 Software.

Author Manuscript Author Manuscript Author Manuscript Author Manuscript

Results

Evaluation of Ron/Met kinase inhibitors against sfRon

We utilized two Ron/Met kinase inhibitors in the study: OSI-296 (34) and BMS-777607 (35); the latter compound is now being developed clinically as ASLAN002 by ASLAN Pharmaceuticals. We first tested the ability of OSI-296 or ASLAN002 to inhibit sfRon activity *in vitro* in MCF7-sfRon cells following serum starvation. Within one hour of treatment, both compounds completely inhibited phosphorylation of sfRon in the 0.5-1 μM range and also caused reduction in downstream phosphorylated AKT when higher doses were given over the same time period (Fig. 1A, B) These data are consistent with our previous results showing robust PI3K/AKT activity downstream of sfRon in MCF7 cells (4).

To test whether ASLAN002 or OSI-296 could effectively treat sfRon-expressing tumors *in vivo*, we treated groups of NOD/SCID mice carrying orthotopic MCF7-sfRon tumors with each of these compounds. Drug treatment (or vehicle control) began when tumors reached a volume of 200 mm^3 and continued every other day for 2 weeks. Treatment groups were vehicle control (40% trappsol in PBS) vs. OSI-296 (200 mg/kg) (Fig. 1C) and, in a separate experiment, vehicle control (70% PEG in PBS) vs. ASLAN002 (50 mg/kg) (Fig. 1D). Both compounds exhibited significant tumor growth inhibition in comparison with controls. The published selectivity of ASLAN002 for Ron kinase (35), and its comparable *in vivo* efficacy to OSI-296 at a 4-fold lower dose (Fig. 1C, D) compelled us to further continue our studies with ASLAN002.

Evaluation of PI3K inhibitors as agents targeting sfRon downstream signaling

To target the PI3K pathway (36), we obtained the pan-PI3K inhibitor NVP-BKM120 and dual PI3K/mTOR inhibitor NVP-BEZ235 from Novartis. We first assessed the activity of NVP-BKM120 and NVP-BEZ235 *in vitro* in MCF7-sfRon cells. We found that both agents were potent inhibitors of PI3K signaling, as determined by dose-dependent inhibition of phosphorylated AKT; however, at higher doses NVP-BEZ235 led to some returning AKT phosphorylation (Fig. 1E). This activity of NVP-BEZ235 has been also reported by others; at certain doses and exposure times the drug may relieve feedback inhibition, resulting in reactivation of PI3K-AKT signaling (37, 38).

We next compared the efficacy of NVP-BKM120 and NVP-BEZ235 against MCF7-sfRon tumors *in vivo* in NOD/SCID mice. Once tumor xenografts reached 200 mm^3, mice were treated daily with vehicle control (10% NMP + 90% PEG300), NVP-BKM120 (60 mg/kg/day) or NVP-BEZ235 (45 mg/kg/day) for 19 days. Both PI3K inhibitors significantly inhibted growth of sfRon-expressing tumors; however, suppression of tumor growth with NVP-BKM120 was significantly better than with NVP-BEZ235 treatment (Fig. 1F). Together, these data provided strong rationale to further pursue NVP-BKM120 in combination with the Ron kinase inhibitor for breast tumors overexpressing sfRon.

Evaluation of Ron and PI3 kinase inhibitors in MCF7-sfRon xenograft model

We next tested ASLAN002 and NVP-BKM120 head-to-head as single agents and as combination therapy against MCF7-sfRon tumors. As a negative control, we included a

Author Manuscript Author Manuscript Author Manuscript Author Manuscript

cohort of mice treated with IMC-RON8, a humanized monoclonal antibody against Ron being investigated in clinical trials [16]. This antibody can inhibit full length Ron, but cannot inhibit sfRon, because sfRon lacks the extracellular domain containing the targeted epitope. We orthotopically transplanted MCF7-sfRon cells into cleared mammary fat pads of NOD/SCID mice and begin treatment when tumors reached a volume of 200 mm^3. Animals were treated for 3 weeks (orally, every other day) with either a vehicle control (70% PEG in PBS), ASLAN002 (50 mg/kg), NVP-BKM120 (60 mg/kg), ASLAN002 + NVP-BKM120 (50 mg/kg, 60 mg/kg, respectively), or animals received IP injection of IMC-RON8 (40 mg/kg) 3 times a week. We found that, although monotherapy with either ASLAN002 or NVP-BKM120 significantly inhibited tumor growth, the most effective treatment regimen was ASLAN002 + NVP-BKM120 combination therapy (Fig. 2A). The results also showed that, as expected, IMC-RON8 was not effective in blocking growth of tumors driven by sfRon. Thus, either Ron kinase inhibition or PI3K inhibition effectively reduces progression of sfRon-expressing MCF7 tumors, but the most powerful effect is achieved with combination therapy. No overt toxicity or weight loss was observed in mice treated with the combination therapy.

Evaluation of the Ron kinase inhibitor ASLAN002 in tumors lacking Ron/sfRon expression

To determine whether ASLAN002 had off-target effects on tumor growth in our models, we conducted a negative control by testing ASLAN002 on a PDX model that does not express Ron receptors. Fresh PDX tumor fragments of HCI-002, which expresses little/no sfRon and Ron (Fig. 2B) were implanted orthtopically into cleared mammary fat pads of NOD/SCID mice. As in the other studies, treatment began when tumors reached a volume of 100 mm^3, and animals were treated orally every other day for 5 weeks with vehicle control (70% PEG in PBS) or ASLAN002 (50 mg/kg). The results showed that ASLAN002 had no effect on tumor growth inhibition in a PDX that does not express appreciable amounts of Ron (Fig. 2C).

Effects of Ron and PI3K inhibition in MCF7-sfRon cells expressing different PI3K variants

MCF7 cells contain a heterozygous mutation in the *PIK3CA* gene (E545K) that could affect the efficacy of Ron or PI3K inhibitors. To determine whether ASLAN002 or NVP-BKM120 have selective effects depending on *PIK3CA* mutation status, we generated stable isogenic MCF7-sfRon cell lines whereby the endogenous *PIK3CA* mRNA was knocked down (Fig. 3A). We then rescued expression of PI3K with a Tet-On system that allowed conditional re-expression of either wild-type (WT) *PIK3CA* cDNA or *PIK3CA* cDNA harboring two of the most common mutations found in human breast tumors, E545K or H1047R (hereafter called PI3K-WT, PI3K-E545K or PI3K-H1047R cell lines, respectively). Addition of doxycycline to the medium induced expression of each rescue variant of PI3K, and induced pAKT to levels that were comparable to that of parental MCF7-sfRon cells (Fig. 3A).

To determine the effect of ASLAN002 or NVP-BKM120 on sfRon-expressing cells with different PI3K alleles, each of the PI3K-inducible cell lines were serum-starved for 24 h, treated with each drug for 1 h, and then evaluated by Western blot for target inhibiton. Results showed that 0.5 μM ASLAN002 completely inhibited active (phosphorylated) sfRon in all cell lines. Higher doses of ASLAN002 (beginning at 1 μM) also inhibited AKT

Author Manuscript Author Manuscript Author Manuscript Author Manuscript

phosphorylation, with the WT PI3K line showing the best effect. sfRon-expressing cells with mutant PI3K required slighly higher doses of ASLAN002 to detect an effect on AKT phosphorylation (Fig. 3B). These findings indicated that mutated PI3K activity may not be completely dependent on sfRon signaling.

We also addressed the impact of mutational status of PI3K on treatment with NVP-BKM120. MCF7-sfRon cells expressing different variants of PI3K and treated with NVP-BKM120 showed good inhibition of AKT phosphorylation regardless of which PI3K variant was expressed (Fig. 3C).

MCF7-sfRon cells expressing different PI3K variants are equally sensitive to Ron and PI3K inhibitors

We next examined the effects of Ron and/or PI3K inhibitors on the viability of sfRon-expressing cells expressing different PI3K variants. Cells were exposed to various concentrations of each drug for four days in high and low cell culture density conditions, since it has been previously reported that cell density may affect drug response and resistance (39). Next, cell survival was estimated using 3-(4,5-dimethylthiazol-2-yl)-2,5-diphenyltetrazolium bromide (MTT). We determined the half maximal effective concentration of each drug (EC_{50}), defined as the concentration of drug that caused 50% loss of cell viability.

Although we observed stronger effects (lower EC50 values) of NVP-BKM120 and/or ASLAN002 on MCF7-sfRon cells viability in high vs. low cell culture density (Fig. 4), the effects of neither compound were significantly affected by PI3K mutation status (Fig. 4). We observed no benefit to adding ASLAN002 to NVP-BKM120 in the *in vitro* cell viability assay, regardless of cell culture density or *PIK3CA* mutation (Fig. 4).

Our data indicate that, *in vitro*, sub-confluent MCF7-sfRon cells were less sensitive to pharmacological treatments than confluent cells, and that the effects of Ron and/or PI3K inhibitors are not strongly affected by *PIK3CA* mutational status of sfRon-expressing MCF7 cells regardless of cell culture density. We next sought to examine Ron and PI3K inhibitors in more physiologically-relevant, non-engineered models of breast cancer *in vivo*.

Evaluation of single agent and dual Ron and PI3K inhibition in breast PDX models expressing endogenous sfRon and WT or mutated *PIK3CA*

To test the potential benefit of Ron and PI3K inhibition in the highest fidelity models possible, we utilized PDX models with or without spontaneous *PIK3CA* mutation. PDX tumors, like human breast tumors, express both endogenous Ron and sfRon (4). We chose four PDX models for our studies: two containing WT *PIK3CA* (HCI-007 and HCI-011) and another two harboring a *PIK3CA* H1047R mutation (HCI-003 and HCI-013). Our models were derived from invasive ductal carcinomas that were estrogen receptor positive and responsive to estrogen (28) (Supplementary Fig. 2) and thus represent the most common type of breast cancer. HCI-007 is the only PDX model used in this study with HER amplifiction (28). As expected based on *PIK3CA* mutation status, HCI-003 and HCI-013 displayed a significantly higher level of phosphorylated AKT than did HCI-007 or HCI-011

Author Manuscript Author Manuscript Author Manuscript Author Manuscript

(Fig. 5A). HCI-013 exhibits the highest level of sfRon expression; sfRon is lower in HCI-003 and HCI-007 PDXs and the lowest in HCI-011 PDX (Fig. 5A).

Fresh PDX tumor fragments were implanted orthtopically into cleared mammary fat pads of NOD/SCID mice. Treatment began when tumors reached a volume of ~100 mm^3, and animals were treated every other day for 4 weeks. Treatment groups consisted of vehicle control (70% PEG in PBS), ASLAN002, NVP-BKM120 or NVP-BKM120 + ASLAN002 combination therapy, using the same doses via oral delivery as in Fig. 2A.

In all four PDX models, treatment with either ASLAN002 alone, NVP-BKM120 alone, or the combination therapy significantly inhibited tumor growth when compared to the vehicle control group. To ensure pharmacological efficacy of inhibitors, we performed pharmacodynamic analysis of sfRon and PI3K signaling within tumors by examining the phosphorylation status of sfRon and AKT (Ser473). As another indicator of AKT activity, we also examined phosphorylation of the PRAS40 protein, which is a demonstrated direct target of AKT (40). The results confirmed reduction of phosphorylated sfRon and Akt, as well as loss of phospho-PRAS40 *in vivo* (Fig. 6A and D). In addition, treatment with ASLAN002 reduces the binding of the p85α subunit of PI3K to sfRon in MCF7 cells and PDX models (Supplemenatry Fig. 3).

Our data also revealed that HCI-007 and HCI-011 (WT *PIK3CA*) showed an excellent initial response to ASLAN002, with tumors initially shrinking in size and then starting to slowly recover (Fig. 5C, D). In contrast, HCI-003 and HCI-013 (*PIK3CA* mutant) responded to ASLAN002 to a lesser extent, with no tumor shrinkage and less effective growth inhibiton over the course of treatment (Fig. 5B, E). Inhibition of PI3K activity with NVP-BKM120 resulted in strong tumor growth inhibition in all four PDX models, and there was no significant benefit to combination therapy for the initial response (see below for data regarding duration of response).

To assess tumor morphology and determine whether treatment with Ron and/or PI3K inhibitors resulted in inhibition of cell proliferation and/or enhancement of apoptosis, we performed H&E and IHC anlysis of representative PDX tumors expressing WT or mutated PI3K (HCI-011 and HCI-013, respectively) with the following antibodies: human cytokeratin (CK), Ki67, and cleaved caspase-3 (Fig. 6B, C, E and F). Overall, there was a good correlation between expression of the proliferation marker Ki67 and tumor growth *in vivo* (Fig. 6C and F). In both tumor models, Ki67 staining decreased markedly upon ASLAN002 and/or NVP-BKM120 treatment in comparison with vehicle-treated tumors. Amongst the different treatment regimens, we observed a significantly higher number of Ki67-positive cells in ASLAN002-treated vs. NVP-BKM120- or combination therapy-treated HCI-013 (PI3K mutant) tumors. This difference was insignificant in HCI-011 (WT PI3K) tumors, which might explain better responses of HCI-011 to ASLAN002 (Fig. 6C and F).

Assessment of apoptosis associated with targeted therapy revealed that vehicle-treated HCI-011 and HCI-013 tumors did not exhibit detectable levels of the apoptotic marker cleaved caspase-3; in contrast, treatment with Ron and/or PI3K inhibitors resulted in various

Author Manuscript Author Manuscript Author Manuscript Author Manuscript

levels of apoptosis (as assessed by percentage of cleaved caspase-3 positive cells). HCI-013 showed minimal overall apoptosis with any treatment (0.1 – 1.9 % of cleaved caspase-3 positive cells). In contrast, HCI-011 was very sensitive to treatment-induced cell death (17.9 – 26.3 % of cleaved caspase-3 positive cells), but with no difference in percentage of apoptotic cells between treatment groups (Fig. 6C and F).

In summary, although we found no differences in the ability of ASLAN002 to affect viability of sfRon-expressing breast cancer cell lines with different PI3K variants *in vitro*, we observed a significant differential effect of ASLAN002 efficacy in four PDX models, which correlated to PI3K mutational status *in vivo*. In particular, we found that treatment with ASLAN002 resulted in stronger inhibition of tumor cell proliferation of PDX tumor that harbor WT PI3K compared to those containing mutated PI3K (Fig. 6C and F).

One theoretical advantage to upfront combination therapy might be prevention of acquired resistance to Ron inhibitors through downstream activation of the PI3K pathway. To address this question, we monitored the residual tumors for three weeks following discontinuation of all treatment. Our data demonstrate that mice bearing HCI-007 or HCI-011 tumors (WT *PIK3CA*) treated previously with combination therapy showed no cancer progression in comparison with mice treated with single agents, whose tumors started to recur (Fig. 5C and D). In contrast, HCI-003 or HCI-013 tumors (mutant *PIK3CA*) demonstrated tumor progression following treatment cessation regardless of the treatment applied (Fig. 5B and E).

Based on the data presented here, we conclude that **(1)** Ron kinase inhibitors such as ASLAN002 can be effective for killing sfRon-expressing breast tumor cells *in vitro* and inhibiting tumor growth *in vivo* using MCF7 and PDX models; **(2)** ASLAN002 can block PI3K pathway activation and cause cell death in sfRon-expressing cells *in vitro*, irrespective of the *PIK3CA* mutation status of the cells; **(3)** ASLAN002 can be as effective as NVP-BKM120 for inhibiting growth of sfRon-expressing PDX tumors *in vivo* when *PIK3CA* status is wild type; **(4)** in *PIK3CA* mutant PDX tumors expressing sfRon, ASLAN002 was not as effective as NVP-BKM120 for initial response indicating partial resistance to this inhibitor; **(5)** ASLAN002 + NVP-BKM120 combination therapy provided a more durable response than either therapy alone following treatment discontinuation in PDX tumors expressing wild type *PIK3CA*, but not *PIK3CA* mutant. Taken together, our data support the notion of targeting sfRon with Ron kinase inhibitors in breast cancer patients, with the important stipulation that tumors harboring *PIK3CA* mutations may be partially resistant to Ron inhibitor therapy. On the other hand, tumors with wild type *PIK3CA* may have less recurrence following treatment with upfront combination Ron/PI3K inhibitor therapy, compared to the outcome with either drug alone.

Discussion

Breast cancer, like many other types of cancer, is such a heterogeneous disease that improvements to standard care are requiring an unprecedented level of precision, chosing treatment cocktails that match specific features of a tumor (41). Likewise, appropriate patient selection criteria are of utmost importance in clinical trial design.

Author Manuscript Author Manuscript Author Manuscript Author Manuscript

An emerging target of importance in breast tumors is the Ron receptor tyrosine kinase, in part because of its dual role in the tumor and in the tumor microenvironment, where it regulates the anti-tumor immune response (3, 42, 43). Despite the success of the IMC-RON8 inhibitory antibody in preclinical studies using several human cancers (20, 44) and a Phase I clinical trial recently completed, our work showed that breast tumors have a preponderance of active sfRon and therefore would not respond to an antibody targeting the Ron extracellular domain (verified in Fig. 2A). Therefore, we have focused our efforts on investigating Ron kinase inhibitors that could be effective against tumors expressing sfRon and/or Ron. Here, we tested two relatively new Ron/Met kinase inhibitors (OSI-296 and ASLAN002). Based on *in vitro* and *in vivo* evaluation of these compounds, ASLAN002 apeared to be better suited than OSI-296 for the treatment of breast tumors exressing sfRon, due to ASLAN002's higher selectivity towards Ron vs. Met (34, 35), and its higher potency for tumor growth inhibition *in vivo* (Fig. 1C and D). Although ASLAN002 was developed as a Ron/Met kinase inhibitor with ~2-fold stronger selective activity for Ron (IC50 = 1.8 nM) over Met (IC50 = 3.9 nM) (35), it has some inhibitory effect toward other Met superfamily kinases such as Axl, Tyro3 and Mer kinases (35). However, according to RNA sequencing data for each of these kinases in the PDX models examined here, expression of different Met superfamily kinases other than Ron is not consistent with the observed response to ASLAN002 in breast PDX tumors (Supplementary Table 2), which strongly suggests that ASLAN002 is blocking growth of these breast tumors through inhibition of Ron kinase activity.

Although several selective tyrosine kinase inhibitors (TKIs) have marked clinical activity, it is widely recognized that the overall value of these agents is substantially limited by the acquisition of drug resistance (45). Resistance to agents targeting receptor tyrosine kinases often results from continued signaling through the PI3K pathway despite TKI treatment, which is often directly associated with *PIK3CA* or *PTEN* mutations (14–17). Importantly, resistance to TKIs can be overcome by addition of a PI3K pathway inhibitor to re-induce remissions (45). For example, trastuzumab resistance of HER2-driven breast tumors with mutated *PIK3CA* can be overcome by treatment with the PI3K inhibitor GDC-0941 (46). This has important implications for the use of Ron kinase inhibitors, especially since sfRon-expressing breast tumors strongly depend on PI3K signaling (4). Moreover, mutations in *PIK3CA* are among the most frequent mutational events in breast cancer (7).

Here, we tested the PI3K inhibitor NVP-BKM120 as a potential candidate for combination with ASLAN002. The results demonstrated that in either *PIK3CA* wild type or mutated PDX tumors the combination of ASLAN002 and NVP-BKM120, despite inducing significant tumor growth inhibtion, was not superior to monotherapy with NVP-BKM120 for the initial response. Interestingly, in a *PIK3CA* wild type breast PDXs, the benefit of combination therapy was not apparent until treatment stopped, whereby combination treatment led to a more durable response (prolonged tumor stasis following cessation of therapy, Fig. 5C and D). However, in a *PIK3CA* mutant breast PDX tumors, we did not observe benefits of combination therapy, these tumors continued to grow progressively following treatment cessation regardless of the treatment applied (Fig. 5B and E).

Author Manuscript Author Manuscript Author Manuscript Author Manuscript

Rexer et al. conducted a comparable study, where recurrence of HER2 expressing breast xenografts with E542K or H1047R *PIK3CA* mutation were evaluated following 4 weeks of treatment with a combination of trastuzumab, lapatinib and NVP-BKM120. The authors concluded that combination of both HER2 and PI3K inhibitors was effective at preventing tumor regrowth, since tumor recurrence eventually developed in about half of the mice. Those observations are consistent with our present findings that concurent inhibition of an RTK (sfRon) and PI3K in tumors with mutant *PIK3CA* leads to recurrence in some of the mice (4 out of 6 mice for HCI-003; Supplementary Table 1), while the rest of the mice remained in a proloned period of tumor stasis. Interestingly, in our experiments, all the mice bearing HCI-007 and 3 out of 7 mice bearing HCI-011 (wild-type *PIK3CA*) PDX tumors exibited lack of tumor regrowth after combination therapy (Supplementary Table 1).

Based on our PDX-based pre-clinical data and the body of literature currently available, we believe there is strong rationale for clinical testing of Ron kinase inhibitors in patients with breast tumors that express sfRon. This should include screening the tumors for *PIK3CA* mutations; our PDX data suggests that the presence of *PIK3CA* mutation contributes to partial resistance to ASLAN002. We also noted that ability to respond to ASLAN002 is not associated with the intrinsic PDX tumor growth rate. These results also imply that there is limited rationale for using Ron kinase inhibitors in breast cancer patients with mutated PI3K. However, the combination of sfRon and PI3K therapies upfront, if risk for toxicity is acceptable, might provide an optimal treatment strategy for patients with wild-type *PIK3CA*. It is noteworthy, however, that the combination of ASLAN002 and NVP-BKM120, despite inducing significant tumor growth inhibtion, was unable to achieve complete and sustained tumor regression in tumor models examined in this study, which is a common feature of targeted therapies (47, 48). Consequently, it may be necessary to combine or otherwise include convetional chemotherapy with sfRon-PI3K-directed targeted therapy for maximal clinical efficacy.

We recognize that there are limitations to this pre-clinical study; the heterogeneity of tumors makes it impossible to generalize from the five models tested here (MCF7-sfRon cells and four sfRon-expressing PDX tumors) to the human breast cancer patients that might be treated with newly emerging Ron inhibitors. However, we believe that this study provides important information relevant to the design of such trials.

Supplementary Material

Refer to Web version on PubMed Central for supplementary material.

Acknowledgments

Financial support:

This work was supported by the National Cancer Institute (7R01CA166422 to ALW), a Susan G. Komen Postdoctoral Fellowship (PDF12230398 to MB) and a research grant from OSI Pharmaceuticals (to ALW).

We thank ASLAN Pharmaceuticals, OSI Pharmaceuticals, Novartis and ImClone LLC for providing drugs for *in vitro* and *in vivo* assays. We thank the Cancer Tissue Pathology core at the Stephenson Cancer Center, University of Oklahoma Health Sciences Center for processing tumor tissues and conducting IHC staining. We are grateful to Trudy Oliver (Huntsman Cancer Institute, Salt Lake City, Utah, USA) for the lentiviral expression vector

Author Manuscript Author Manuscript Author Manuscript Author Manuscript

pLentiTRE/rtTA and Jeff Hager (Seragon Pharmaceuticals, San Diego, CA) for providing us with data regarding characterization of beeswax E2 pellets. We also wish to thank our colleagues Guoying Wang, Yoko DeRose, Yi-Chun (Christine) Lin, and Jin Liu for help developing and maintaining PDX tumors and animals.

References

1. Welm AL, Sneddon JB, Taylor C, Nuyten DS, van de Vijver MJ, Hasegawa BH, et al. The macrophage-stimulating protein pathway promotes metastasis in a mouse model for breast cancer and predicts poor prognosis in humans. Proc Natl Acad Sci U S A. 2007; 104(18):7570–5. [PubMed: 17456594]
2. Cunha S, Lin YC, Goossen EA, Devette CI, Albertella MR, Thomson S, et al. The RON Receptor Tyrosine Kinase Promotes Metastasis by Triggering MBD4-Dependent DNA Methylation Reprogramming. Cell Rep. 2014; 6(1):141–54. [PubMed: 24388747]
3. Kretschmann KL, Eyob H, Buys SS, Welm AL. The macrophage stimulating protein/Ron pathway as a potential therapeutic target to impede multiple mechanisms involved in breast cancer progression. Curr Drug Targets. 2010; 11(9):1157–68. [PubMed: 20545605]
4. Liu X, Zhao L, Derose YS, Lin YC, Bieniasz M, Eyob H, et al. Short-Form Ron Promotes Spontaneous Breast Cancer Metastasis through Interaction with Phosphoinositide 3-Kinase. Genes Cancer. 2011; 2(7):753–62. [PubMed: 22207901]
5. Angeloni D, Danilkovitch-Miagkova A, Ivanova T, Braga E, Zabarovsky E, Lerman MI. Hypermethylation of Ron proximal promoter associates with lack of full-length Ron and transcription of oncogenic short-Ron from an internal promoter. Oncogene. 2007; 26(31):4499–512. [PubMed: 17297469]
6. Mills GB, Kohn E, Lu Y, Eder A, Fang X, Wang H, et al. Linking molecular diagnostics to molecular therapeutics: targeting the PI3K pathway in breast cancer. Semin Oncol. 2003; 30(5 Suppl 16):93–104. [PubMed: 14613030]
7. Li SY, Rong M, Grieu F, Iacopetta B. PIK3CA mutations in breast cancer are associated with poor outcome. Breast Cancer Res Treat. 2006; 96(1):91–5. [PubMed: 16317585]
8. Campbell IG, Russell SE, Choong DY, Montgomery KG, Ciavarella ML, Hooi CS, et al. Mutation of the PIK3CA gene in ovarian and breast cancer. Cancer Res. 2004; 64(21):7678–81. [PubMed: 15520168]
9. Buttitta F, Felicioni L, Barassi F, Martella C, Paolizzi D, Fresu G, et al. PIK3CA mutation and histological type in breast carcinoma: high frequency of mutations in lobular carcinoma. J Pathol. 2006; 208(3):350–5. [PubMed: 16353168]
10. Carson JD, Van Aller G, Lehr R, Sinnamon RH, Kirkpatrick RB, Auger KR, et al. Effects of oncogenic p110alpha subunit mutations on the lipid kinase activity of phosphoinositide 3-kinase. Biochem J. 2008; 409(2):519–24. [PubMed: 17877460]
11. Samuels Y, Diaz LA Jr, Schmidt-Kittler O, Cummins JM, Delong L, Cheong I, et al. Mutant PIK3CA promotes cell growth and invasion of human cancer cells. Cancer Cell. 2005; 7(6):561–73. [PubMed: 15950905]
12. Saal LH, Johansson P, Holm K, Gruvberger-Saal SK, She QB, Maurer M, et al. Poor prognosis in carcinoma is associated with a gene expression signature of aberrant PTEN tumor suppressor pathway activity. Proc Natl Acad Sci U S A. 2007; 104(18):7564–9. [PubMed: 17452630]
13. Janku F, Tsimberidou AM, Garrido-Laguna I, Wang X, Luthra R, Hong DS, et al. PIK3CA mutations in patients with advanced cancers treated with PI3K/AKT/mTOR axis inhibitors. Mol Cancer Ther. 2011; 10(3):558–65. [PubMed: 21216929]
14. Berns K, Horlings HM, Hennessy BT, Madiredjo M, Hijmans EM, Beelen K, et al. A functional genetic approach identifies the PI3K pathway as a major determinant of trastuzumab resistance in breast cancer. Cancer Cell. 2007; 12(4):395–402. [PubMed: 17936563]
15. Chandarlapaty S, Sakr RA, Giri D, Patil S, Heguy A, Morrow M, et al. Frequent mutational activation of the PI3K-AKT pathway in trastuzumab-resistant breast cancer. Clin Cancer Res. 2012; 18(24):6784–91. [PubMed: 23092874]
16. Eichhorn PJ, Gili M, Scaltriti M, Serra V, Guzman M, Nijkamp W, et al. Phosphatidylinositol 3-kinase hyperactivation results in lapatinib resistance that is reversed by the mTOR/

Author Manuscript Author Manuscript Author Manuscript Author Manuscript

phosphatidylinositol 3-kinase inhibitor NVP-BEZ235. Cancer Res. 2008; 68(22):9221–30. [PubMed: 19010894]

17. Yuan TL, Cantley LC. PI3K pathway alterations in cancer: variations on a theme. Oncogene. 2008; 27(41):5497–510. [PubMed: 18794884]
18. Alvarez RH. Present and future evolution of advanced breast cancer therapy. Breast Cancer Res. 2010; 12 (Suppl 2):S1. [PubMed: 21050422]
19. Yao HP, Zhou YQ, Ma Q, Guin S, Padhye SS, Zhang RW, et al. The monoclonal antibody Zt/f2 targeting RON receptor tyrosine kinase as potential therapeutics against tumor growth-mediated by colon cancer cells. Mol Cancer. 2011; 10:82. [PubMed: 21749705]
20. O'Toole JM, Rabenau KE, Burns K, Lu D, Mangalampalli V, Balderes P, et al. Therapeutic implications of a human neutralizing antibody to the macrophage-stimulating protein receptor tyrosine kinase (RON), a c-MET family member. Cancer Res. 2006; 66(18):9162–70. [PubMed: 16982759]
21. Molife LR, Dean EJ, Blanco-Codesido M, Krebs MG, Brunetto AT, Greystoke AP, et al. A Phase I, Dose-Escalation Study of the Multitargeted Receptor Tyrosine Kinase Inhibitor, Golvatinib, in Patients with Advanced Solid Tumors. Clin Cancer Res. 2014
22. Guin S, Yao HP, Wang MH. RON receptor tyrosine kinase as a target for delivery of chemodrugs by antibody directed pathway for cancer cell cytotoxicity. Mol Pharm. 2010; 7(2):386–97. [PubMed: 20039696]
23. Wang MH, Padhye SS, Guin S, Ma Q, Zhou YQ. Potential therapeutics specific to c-MET/RON receptor tyrosine kinases for molecular targeting in cancer therapy. Acta Pharmacol Sin. 2010; 31(9):1181–8. [PubMed: 20694025]
24. Kola I, Landis J. Can the pharmaceutical industry reduce attrition rates? Nat Rev Drug Discov. 2004; 3(8):711–5. [PubMed: 15286737]
25. Hait WN. Anticancer drug development: the grand challenges. Nat Rev Drug Discov. 2010; 9(4): 253–4. [PubMed: 20369394]
26. Clarke R. The role of preclinical animal models in breast cancer drug development. Breast Cancer Res. 2009; 11 (Suppl 3):S22. [PubMed: 20030874]
27. Kao J, Salari K, Bocanegra M, Choi YL, Girard L, Gandhi J, et al. Molecular profiling of breast cancer cell lines defines relevant tumor models and provides a resource for cancer gene discovery. PLoS One. 2009; 4(7):e6146. [PubMed: 19582160]
28. DeRose YS, Wang G, Lin YC, Bernard PS, Buys SS, Ebbert MT, et al. Tumor grafts derived from women with breast cancer authentically reflect tumor pathology, growth, metastasis and disease outcomes. Nat Med. 2011; 17(11):1514–20. [PubMed: 22019887]
29. Sikora MJ, Cooper KL, Bahreini A, Luthra S, Wang G, Chandran UR, et al. Invasive lobular carcinoma cell lines are characterized by unique estrogen-mediated gene expression patterns and altered tamoxifen response. Cancer Res. 2014; 74(5):1463–74. [PubMed: 24425047]
30. DeRose, YS.; Gligorich, KM.; Wang, G.; Georgelas, A.; Bowman, P.; Courdy, SJ., et al. Patient-derived models of human breast cancer: protocols for in vitro and in vivo applications in tumor biology and translational medicine. In: Enna, SJ., editor. Current protocols in pharmacology/ editorial board. Vol. Chapter 14. 2013. p. 23
31. Zufferey R, Nagy D, Mandel RJ, Naldini L, Trono D. Multiply attenuated lentiviral vector achieves efficient gene delivery in vivo. Nat Biotechnol. 1997; 15(9):871–5. [PubMed: 9306402]
32. Maira SM, Pecchi S, Huang A, Burger M, Knapp M, Sterker D, et al. Identification and characterization of NVP-BKM120, an orally available pan-class I PI3-kinase inhibitor. Mol Cancer Ther. 2012; 11(2):317–28. [PubMed: 22188813]
33. Mezei TSM, Dénes L, Jung J. Egyed-Zsigmond Semiautomated Image Analysis of High Contrast Tissue Areas Using Hue/Saturation/Brightness Based Color Filtering. Acta Medica Marisiensis. 2011; 57(6):679–84.
34. Steinig AG, Li AH, Wang J, Chen X, Dong H, Ferraro C, et al. Novel 6-aminofuro[3,2-c]pyridines as potent, orally efficacious inhibitors of cMET and RON kinases. Bioorganic & medicinal chemistry letters. 2013; 23(15):4381–7. [PubMed: 23773865]
35. Schroeder GM, An Y, Cai ZW, Chen XT, Clark C, Cornelius LA, et al. Discovery of N-(4-(2-amino-3-chloropyridin-4-yloxy)-3-fluorophenyl)-4-ethoxy-1-(4-fluorophenyl)-2-oxo-1,2-

Author Manuscript Author Manuscript Author Manuscript Author Manuscript

dihydropyridine-3-carboxamide (BMS-777607), a selective and orally efficacious inhibitor of the Met kinase superfamily. J Med Chem. 2009; 52(5):1251–4. [PubMed: 19260711]

36. Markman B, Dienstmann R, Tabernero J. Targeting the PI3K/Akt/mTOR pathway--beyond rapalogs. Oncotarget. 2010; 1(7):530–43. [PubMed: 21317449]
37. Tanaka H, Yoshida M, Tanimura H, Fujii T, Sakata K, Tachibana Y, et al. The selective class I PI3K inhibitor CH5132799 targets human cancers harboring oncogenic PIK3CA mutations. Clin Cancer Res. 2011; 17(10):3272–81. [PubMed: 21558396]
38. Lin A, Piao HL, Zhuang L, Sarbassov DD, Ma L, Gan B. FoxO Transcription Factors Promote AKT Ser473 Phosphorylation and Renal Tumor Growth in Response to Pharmacologic Inhibition of the PI3K-AKT Pathway. Cancer Res. 2014
39. de Anta JM, Real FX, Mayol X. Low tumor cell density environment yields survival advantage of tumor cells exposed to MTX in vitro. Biochim Biophys Acta. 2005; 1721(1–3):98–106. [PubMed: 15652184]
40. Wiza C, Nascimento EB, Ouwens DM. Role of PRAS40 in Akt and mTOR signaling in health and disease. Am J Physiol Endocrinol Metab. 2012; 302(12):E1453–60. [PubMed: 22354785]
41. Trop I, LeBlanc SM, David J, Lalonde L, Tran-Thanh D, Labelle M, et al. Molecular classification of infiltrating breast cancer: toward personalized therapy. Radiographics : a review publication of the Radiological Society of North America, Inc. 2014; 34(5):1178–95.
42. Eyob H, Ekiz HA, Welm AL. RON promotes the metastatic spread of breast carcinomas by subverting antitumor immune responses. Oncoimmunology. 2013; 2(9):e25670. [PubMed: 24327933]
43. Eyob H, Ekiz HA, Derose YS, Waltz SE, Williams MA, Welm AL. Inhibition of ron kinase blocks conversion of micrometastases to overt metastases by boosting antitumor immunity. Cancer Discov. 2013; 3(7):751–60. [PubMed: 23612011]
44. Zou Y, Howell GM, Humphrey LE, Wang J, Brattain MG. Ron knockdown and Ron monoclonal antibody IMC-RON8 sensitize pancreatic cancer to histone deacetylase inhibitors (HDACi). PLoS One. 2013; 8(7):e69992. [PubMed: 23922886]
45. Engelman JA, Settleman J. Acquired resistance to tyrosine kinase inhibitors during cancer therapy. Curr Opin Genet Dev. 2008; 18(1):73–9. [PubMed: 18325754]
46. Junttila TT, Akita RW, Parsons K, Fields C, Lewis Phillips GD, Friedman LS, et al. Ligand-independent HER2/HER3/PI3K complex is disrupted by trastuzumab and is effectively inhibited by the PI3K inhibitor GDC-0941. Cancer Cell. 2009; 15(5):429–40. [PubMed: 19411071]
47. Garcia-Garcia C, Ibrahim YH, Serra V, Calvo MT, Guzman M, Grueso J, et al. Dual mTORC1/2 and HER2 blockade results in antitumor activity in preclinical models of breast cancer resistant to anti-HER2 therapy. Clin Cancer Res. 2012; 18(9):2603–12. [PubMed: 22407832]
48. Courtney KD, Corcoran RB, Engelman JA. The PI3K pathway as drug target in human cancer. J Clin Oncol. 2010; 28(6):1075–83. [PubMed: 20085938]

Author Manuscript Author Manuscript Author Manuscript Author Manuscript

Translational Relevance

Using PDX models, which are arguably the most clinically-relevant models of human breast cancer, this work provides pre-clinical rationale for future clinical testing of Ron kinase inhibitors in patients with breast tumors that express sfRon. Our results indicate that such trials should include screening tumors for *PIK3CA* mutations; our PDX data showed that the presence of *PIK3CA* mutation contributes to partial resistance to the Ron inhibitor ASLAN002. Therefore, there is limited rationale for using Ron kinase inhibitors in breast cancer patients with mutated PI3K. In tumors with wild-type *PIK3CA*, the upfront combination of sfRon and PI3K inhibitors, may provide the optimal treatment strategy; we found that durable tumor stasis was sustained even after treatment was discontinued.

Author Manuscript
Author Manuscript
Author Manuscript
Author Manuscript

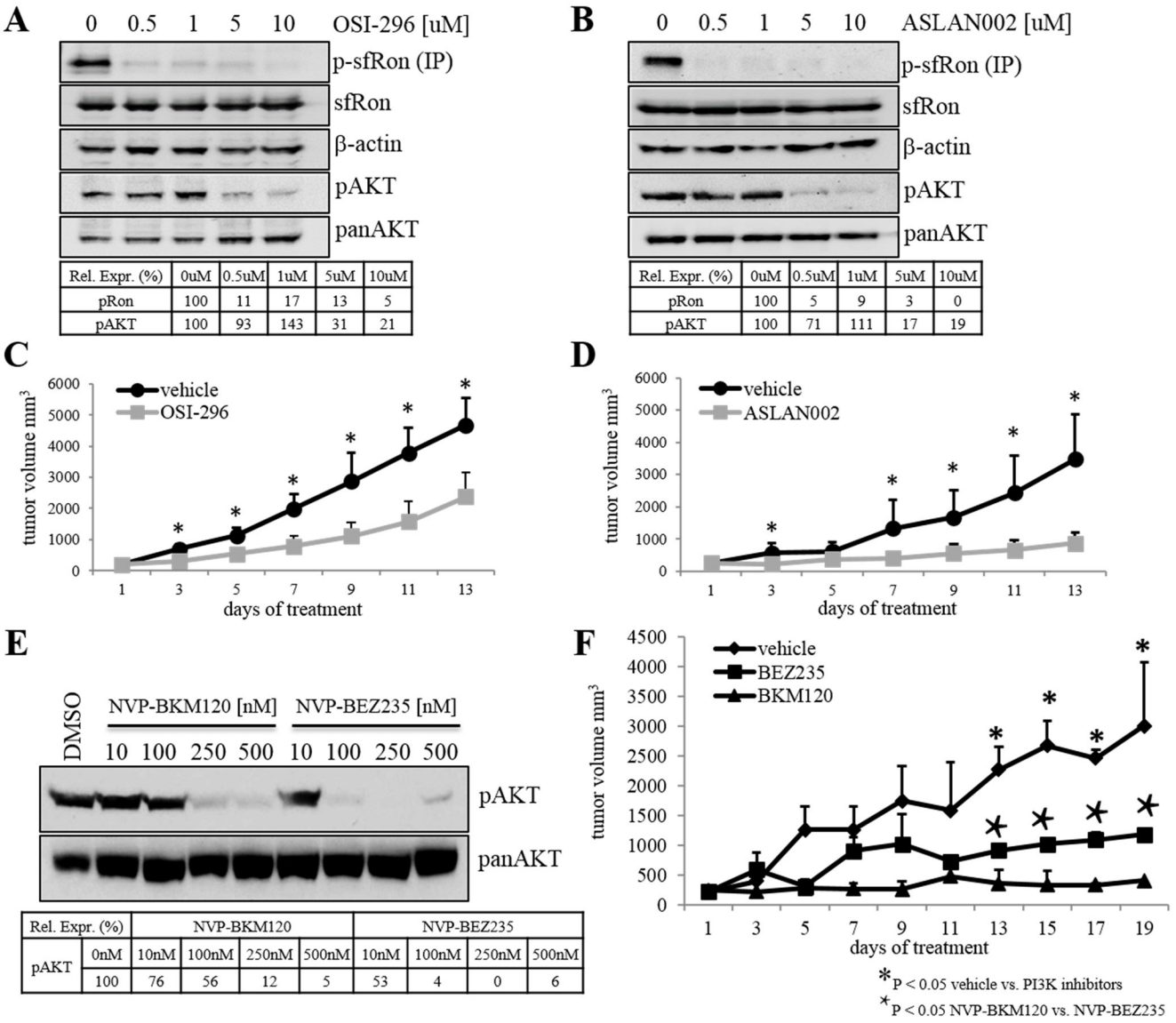

Rel. Expr. (%)	0uM	0.5uM	1uM	5uM	10uM
pRon	100	11	17	13	5
pAKT	100	93	143	31	21

Rel. Expr. (%)	0uM	0.5uM	1uM	5uM	10uM
pRon	100	5	9	3	0
pAKT	100	71	111	17	19

Rel. Expr. (%)	NVP-BKM120					NVP-BEZ235			
pAKT	0nM	10nM	100nM	250nM	500nM	10nM	100nM	250nM	500nM
	100	76	56	12	5	53	4	0	6

Figure 1. The efficacy of Ron and PI3 kinase inhibitors

A. IP-Western blot showing inhibition of phosphorylated (active) sfRon in MCF7-sfRon cells treated with Ron kinase inhibitor OSI-296. The blot was quantified using the ChemiDoc XRS system with Image Lab Software and the table represents percentage of p-sfRon or pAKT expression normalized to total sfRon or AKT protein after treatment with various doses of the drug. **B.** IP-Western blot showing almost complete suppresion of p-sfRon or PI3K signaling in MCF7-sfRon cells by 0.5 or 5 μM concentrations of Ron kinase inhibitor ASLAN002, respectively, which is quantified in the table below. **C–D.** Graphs represent orthotopic MCF7-sfRon tumor growth rate in NOD/SCID mice treated every other day with vehicle (40% trappsol in PBS) or OSI-296 (200 mg/kg) **(C)** and vehicle (70% PEG in PBS) or ASLAN002 (50 mg/kg) **(D)**. Asterisks indicate a statistically significant difference ($p < 0.05$) in tumor growth rate between vehicle and OSI-296 or ASLAN002 treatment groups. **E.** Western blot showing the effect of NVP-BKM120 and NVP-BEZ235

Author Manuscript Author Manuscript Author Manuscript Author Manuscript

on PI3K signaling in MCF7-sfRon cells. Levels of phosphorylated AKT (p-AKT), or total AKT were assessed in the presence of either of these inhibitors. **F.** Graph represents orthotopic MCF7-sfRon tumor growth rate in NOD/SCID mice. Animals were treated daily with vehicle (10% NMP + 90% PEG300), NVP-BKM120 (60 mg/kg) or NVP-BEZ235 (45 mg/kg) beginning when tumors reached a volume of 200 mm^3.

Author Manuscript Author Manuscript Author Manuscript Author Manuscript

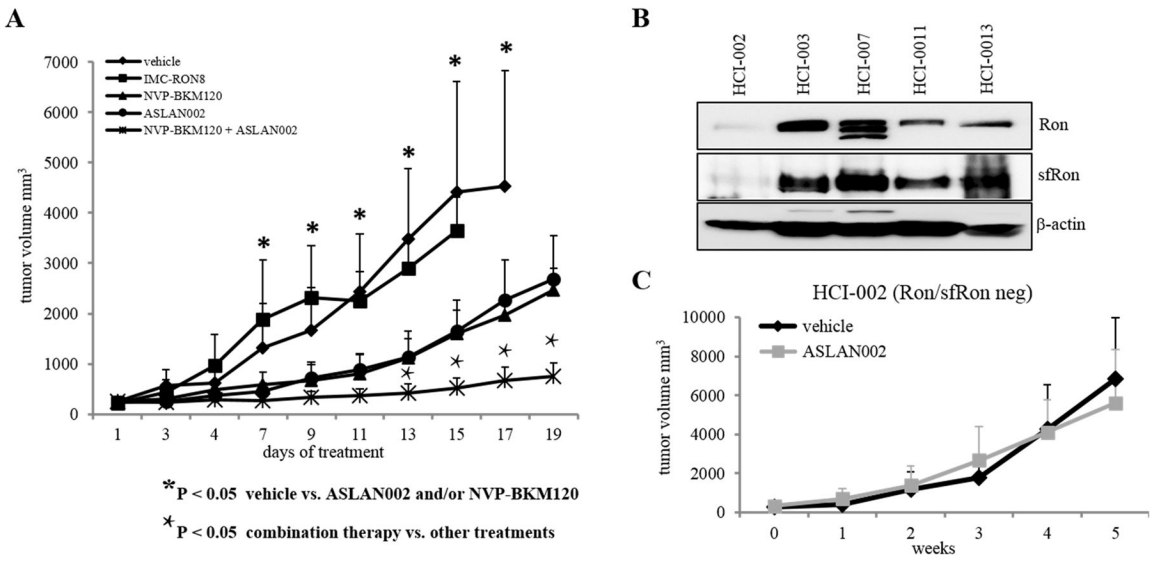

Figure 2. Evaluation of Ron and PI3K inhibitors in MCF7-sfRon xenografts and the HCI-002 (Ron/sfRon negative) breast PDX tumor model

A. Graph represents orthotopic MCF7-sfRon tumor growth rate in NOD/SCID mice treated orally with vehicle (70% PEG in PBS), ASLAN002 (50 mg/kg), NVP-BKM120 (60 mg/kg), ASLAN002 + NVP-BKM120 (50 mg/kg, 60 mg/kg, respectively) every other day, or with IP injections of IMC-RON8 (40 mg/kg) 3 times a week for 19 days, beginning when tumors reached a volume of 200 mm^3. As expected, the IMC-RON8 antibody against Ron (included as negative control) was not effective in blocking growth of tumors driven by sfRon. **B.** Western blot showing levels of sfRon and Ron in a panel of breast PDX models used in this study. HCI-002 is very low or negative for sfRon and Ron expression, in contrast to HCI-003, HCI-007, HCI-011 and HCI-013 PDX tumors that express Ron receptors. **C.** Graph represents orthotopic HCI-002 tumor growth rate in NOD/SCID mice. Animals were treated orally every other day for 5 weeks with vehicle (70% PEG in PBS) or ASLAN002 (50 mg/kg), beginning when tumors reached a volume of 100 mm^3.

Author Manuscript Author Manuscript Author Manuscript Author Manuscript

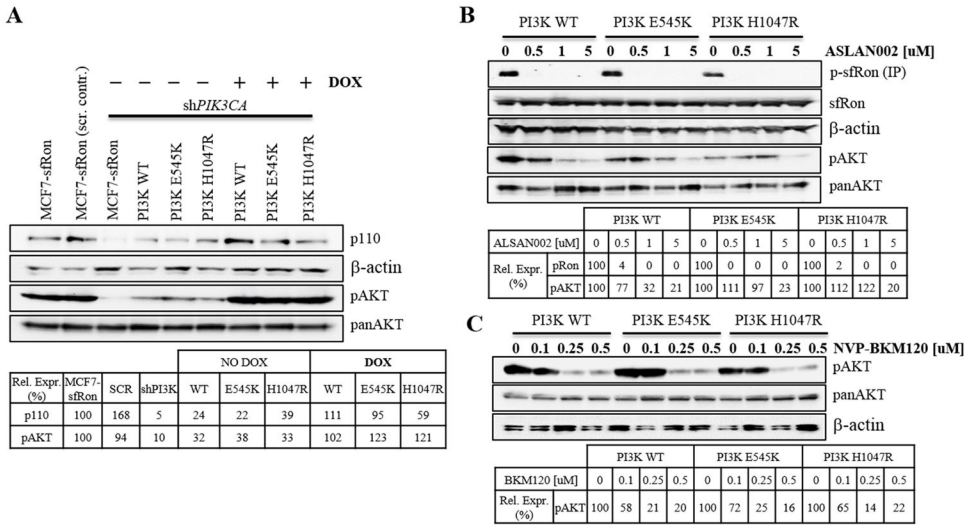

Rel. Expr. (%)	MCF7-sfRon	SCR	shPI3K	NO DOX WT	NO DOX E545K	NO DOX H1047R	DOX WT	DOX E545K	DOX H1047R
p110	100	168	5	24	22	39	111	95	59
pAKT	100	94	10	32	38	33	102	123	121

ALSAN002 [uM]		PI3K WT 0	0.5	1	5	PI3K E545K 0	0.5	1	5	PI3K H1047R 0	0.5	1	5
Rel. Expr. (%)	pRon	100	4	0	0	100	0	0	0	100	2	0	0
	pAKT	100	77	32	21	100	111	97	23	100	112	122	20

BKM120 [uM]		PI3K WT 0	0.1	0.25	0.5	PI3K E545K 0	0.1	0.25	0.5	PI3K H1047R 0	0.1	0.25	0.5
Rel. Expr. (%)	pAKT	100	58	21	20	100	72	25	16	100	65	14	22

Figure 3. The effect of *PIK3CA* activating mutations (E545K and H1047R) on the treatment with ASLAN002 or NVP-BKM120

A. Western blot analysis of PI3K signaling network in MCF7-sfRon cells engineered to conditionally express different alleles of *PIK3CA* gene. First, the endogenous *PIK3CA* mRNA was knocked down in MCF7-sfRon cells (MCF7-sfRon sh*PIK3CA*); shRNA with scrambled sequence served as negative control (MCF7-sfRon scr. contr.). Next, expression of PI3K was rescued with a Tet-On system allowing conditional re-expression of different variants of *PIK3CA* gene (WT, E545K and H1047R). Treatment with doxocycline (DOX, 500 ng/ml) for 24 h led to conditional activation of PI3K reflected as presence of PI3K p110α and pAKT. Cells grown in absence of DOX (despite a small amount of leaky expression from the rescue constructs) showed reduced phosphorylation of AKT. The blot was quantified using ChemiDoc XRS system with Image Lab Software, and the table represents the percentage of p110 and pAKT expression normalized to β-actin or total AKT protein, with or without addition of DOX. **B.** IP-Western blot showing complete inhibition of p-sfRon by 0.5 μM ASLAN002 in either PI3K WT or PI3K mutant MCF7-sfRon cells. Higher doses of ASLAN002 (beginning at 1 μM) also inhibited AKT phosphorylation, with the WT PI3K line showing the best effect, which is quantified in the table. All lanes were treated with 500 ng/ml of DOX 24h before treatment began to induce expression of the desired PI3K construct. **C.** Western blot showing results of the treatment of MCF7-sfRon cells with NVP-BKM120. 0.25 μM dose of PI3K inhibitor was sufficient to suppress pAKT in each cell line regardless of which PI3K variant was expressed, which is quantified in the table. All lanes were treated with 500 ng/ml of DOX 24h before treatment began.

Author Manuscript Author Manuscript Author Manuscript Author Manuscript

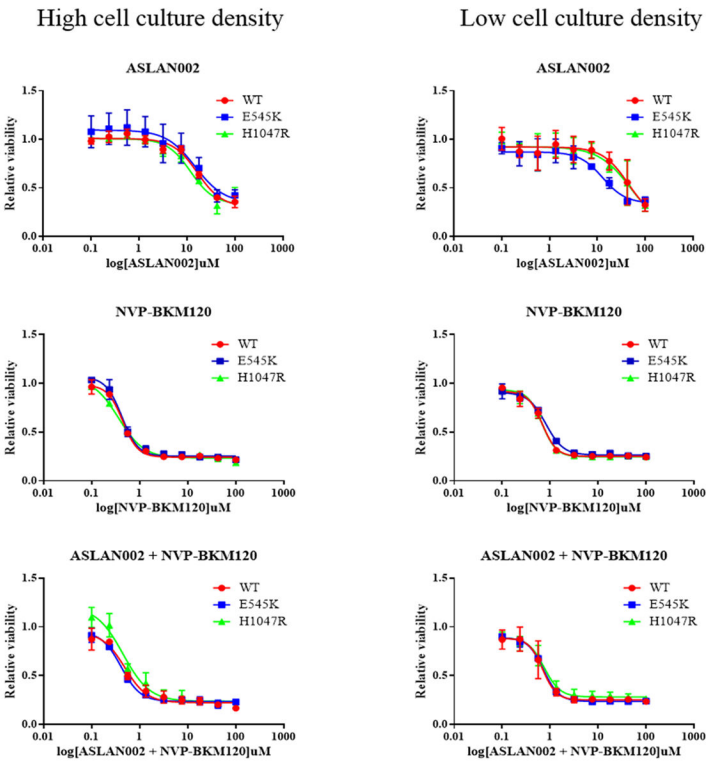

EC50 [μM]	ASLAN002	NVP-BKM120	ASLAN002 + NVP-BKM120
WT	13.81	0.44	0.49
E545K	14.84	0.43	0.41
H1047R	11.89	0.36	0.45

EC50 [μM]	ASLAN002	NVP-BKM120	ASLAN002 + NVP-BKM120
WT	26.24	0.69	0.70
E545K	20.95	0.81	0.73
H1047R	24.46	0.66	0.75

Figure 4. Evaluation of the effect of ASLAN002 and/or NVP-BKM120 on viability of MCF7-sfRon cells expressing different variants of *PIK3CA* gene

Graphs represent relative viability of MCF7-sfRon cells treated for 4 days with a range of drug concentrations (0.1 – 100 μM), in either high (left panel) or low (right panel) density conditions. The EC50 of ASLAN002, NVP-BKM120, or the combination of both drugs was estimated for each cell line and sumarized in tables. Both compounds reduced the viability of MCF7-sfRon cells with a stronger effect (lower values of EC50) in the high density condition, but all lines showed equal sensitivity to NVP-BKM120 and/or ASLAN002.

Author Manuscript Author Manuscript Author Manuscript Author Manuscript

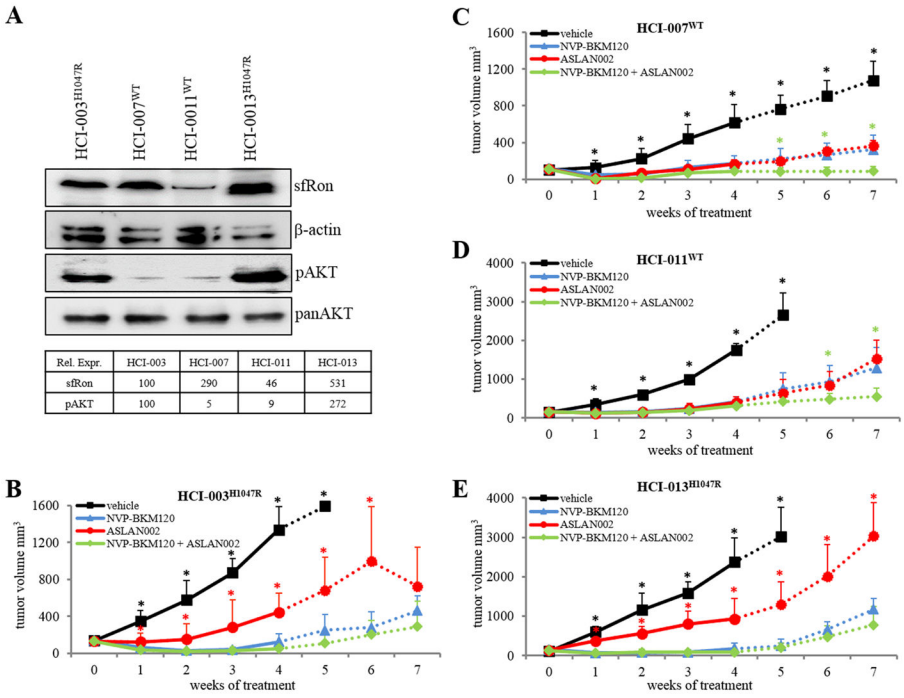

Figure 5. Evaluation of Ron and PI3 kinase inhibitors in breast tumor grafts expressing sfRon and WT or mutated *PIK3CA* gene

A. Western blot showing levels of sfRon and pAKT in four breast PDX models used to test efficacy of Ron and PI3K inhibitors. PDXs containing a spontaneous mutation in *PIK3CA* (HCI-003 and HCI-013) displayed a significantly higher level of phosphorylated AKT than PDXs with WT *PIK3CA* (HCI-007 and HCI-011). **B, E.** Graphs represent orthotopic HCI-003 or HCI-013 tumor growth rate in NOD/SCID mice. Animals were treated orally every other day for 4 weeks with vehicle (70% PEG in PBS), ASLAN002 (50 mg/kg), NVP-BKM120 (60 mg/kg), ASLAN002 + NVP-BKM120 (50 mg/kg, 60 mg/kg, respectively), beginning when tumors reached a volume of 100 mm^3. Treatment was discontinued after 4 weeks and mice were followed for recurrence, in order to investigate the long-term effect of Ron and PI3 kinase inhibitors (indicated as dashed lines on the graph). **C, D.** HCI-007 and HCI-011 tumors were treated as in **B, E. B–E.** Black asterisks indicate a statistically significant difference ($p < 0.05$) in tumor growth between vehicle and all other treatment groups; red asterisks indicate a significant difference between ASLAN002 vs. NVP-BKM120 or combination therapy groups; green asterisks indicate a significant difference between combination therapy vs. either monotherapy.

Author Manuscript Author Manuscript Author Manuscript Author Manuscript

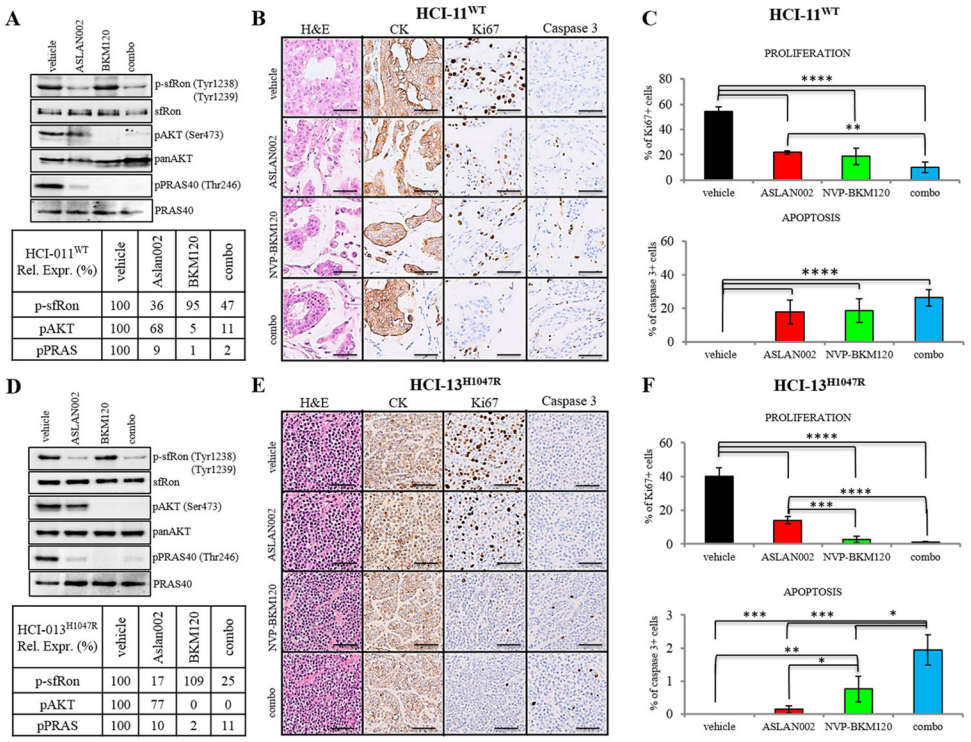

HCI-011^{WT} Rel. Expr. (%)	vehicle	Aslan002	BKM120	combo
p-sfRon	100	36	95	47
pAKT	100	68	5	11
pPRAS	100	9	1	2

HCI-013^{H1047R} Rel. Expr. (%)	vehicle	Aslan002	BKM120	combo
p-sfRon	100	17	109	25
pAKT	100	77	0	0
pPRAS	100	10	2	11

Figure 6. Molecular and IHC analysis of treated breast PDX tumors

A. Representative Western blot showing Ron and/or PI3K inhibitor target inhibition in NOD/SCID mice bearing HCI-011 (*PIK3CA*^{WT}) tumors. The pharmacodynamic effect was measured 3 h following administration of single dose of each drug: ASLAN002 (50 mg/kg), NVP-BKM120 (60 mg/kg) or the combination of these two drugs (combo, ASLAN002 50 mg/kg + NVP-BKM120 60 mg/kg) vs. vehicle. **B.** Representative sections of tumors obtained from therapeutic experiments on HCI-011 (*PIK3CA*^{WT}) treated with different drug regimens. Tumor sections were H&E stained and immunohistochemically evaluated for cytokeratins, Ki67 or cleaved caspase-3 expression. Scale bar = 100 μM **C.** Quantification of Ki67 or cleaved caspase-3 positive cells determined from IHC staining of HCI-011 tumors shown in panel **B. D.** Pharmacodynamic effect of Ron and/or PI3K inhibitors assessed in HCI-013 PDX (*PIK3CA*^{H1047R}) tumor as in **A. E.** Representative sections of tumors obtained from therapeutic experiments on HCI-013 (*PIK3CA*^{H1047R}) treated with different drug regimens. Tumor sections were H&E stained and immunohistochemically evaluated for cytokeratins, Ki67 or cleaved caspase-3 expression. Scale bar = 100 μM. **F.** Quantification of Ki67 or cleaved caspase-3 positive cells determined from IHC staining of HCI-013 tumors shown in **E**.